



Visual SHM for Concrete Infrastructure Using a Wall-climbing Robot

Liang Yang^{1,2}, Yong Chang², Biao Jiang¹, Jizhong Xiao¹

¹ *The Robotics Lab, The City College of New York, New York, USA*

² *Shenyang Institute of Automation, Chinese Academy of Sciences, China*

Abstract

Concrete structural health monitoring (SHM) is urgently required with more and more severe aging problems happen. Conventional manual inspection approach is labor-intensive and time-consuming. In this paper, we propose a wall-climbing robotic approach for visual inspection of concrete structures using a deep neural network and 3D semantic reconstruction to build a 3D map overlaid with defects. The wall-climbing robot uses a negative pressure module to operate on both vertical and horizontal surfaces. An RGB-D camera is mounted in the robot with an Intel-NUC computer as visual positioning and image processing core to make metric measurement, Our main contribution is the inspection neural network that performs pixel-level segmentation to detect cracks and spallings and mark them on a 3D map for better visualization. We build a semantic dataset which includes 820 labeled images and training on the dataset with 12,000 iterations. We introduce a 3D semantic fusion method to build the 3D map with defects highlighted. The field test and experimental results demonstrate that our wall-climbing robot and inspection system can perform a robust 3D metric inspection.

1. Introduction

Structural health monitoring (SHM) plays a significant role on performance evaluation and condition assessments for the Nation's highway transportation assets, and it can promote its operational safety and longevity based on data-driven analysis and decisions. The Federal Highway Administration (FHWA) of the U.S. Department of Transportation (DOT) has launched the Long-Term Bridge Performance (LTBP) Program in 2015 to facilitate the SHM by collecting critical performance data (N.Gucunski 2015). According to the FHWA's latest bridge element inspection manual (F. H. Administration 2014), New York Bridge Inspection Manual (N. Y. D. of Transportation 2016), and Tunnel Operations, Maintenance, Inspection, and Evaluation (TOMIE) Manual (F. H. Administration 2015), it is required to identify, measure, and record the condition state information during a routine inspection on bridges and tunnels. Such condition states include spall (delamination, patched area), exposed rebar, cracking, abrasion (wear), and damage. The spallings and cracks are the main factors affecting the condition states of reinforced concrete (C. Koch and K. Georgieva 2015).

Automated visual inspection (G. Li and S. He 2014), (R. Adhikari and O. Moselhi 2014), (M. R. Jahanshahi and S. F. Masri 2012) has become a popular approach for structural surface inspection with the advance development in optics devices, such as for structural displacement measurement, crack or spalling inspection. Several robotic inspection systems have been

developed for automated visual inspection data collection and processing. Researchers in Rutgers University developed a mobile robotic crack inspection and mapping system, and it uses edge detection algorithms to detect the cracks on concrete bridge decks and generate the crack map for bridge maintenance (R. S. Lim 2014). Under the support of FHWA LTBP program, an autonomous bridge deck inspection mobile robotic system has been developed with visual cameras and other detection sensors (P. Prasanna 2016), (H. M. La 2017). Unmanned aerial vehicle (UAV) has also been deployed for bridge visual inspection (N. Hallermann 2014). Our previous wall-climbing robot is proved to be able to provide vertical mobility to perform visual inspection and GPR-based subsurface flaw inspection (B. Li 2017). However, it is still a challenging and unsolved problem to empower the robots with metric visual inspection capability.

In this paper, we aim to: (i) design, build, and test wall-climbing robots to carry cameras for visual inspection of surface flaws, (ii) investigate visual inspection methods and image processing algorithms to identify, measure and record the condition state information of bridge structure members, (iii) investigate motion control and V-SLAM (visual simultaneous localization and mapping) methods to localize defect locations and register them in 3D model for better visualization, (vi) demonstrate the field performance of the integrated robotic inspection system at bridge sites.

2. Wall-climbing Robot System Architecture

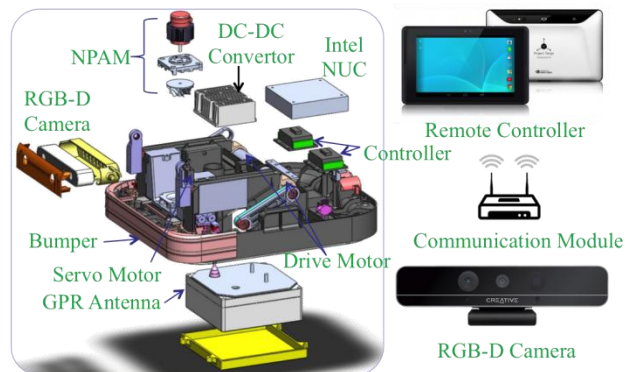


Fig. 1 The electrical components and sensors in wall-climbing robot.

We produce a wall-climbing robot prototype as shown in Fig.1. It consists of a negative pressure adhesive module (NPAM), a pressure sensor, two drive wheels and the associated motors and controllers, one servo motor to adjust the camera tilt angle, a bumper, a DC-DC converter, an Intel NUC computer for on-board image/signal processing. It maintains a constant negative pressure inside a suction chamber by adjusting the propeller speed of the NPAM to achieve a desirable balance of strong adhesion and high mobility. Since it doesn't require perfect sealing as vacuum suction techniques would, it can thus move on both smooth and rough surfaces, and cross over shallow grooves. It carries a RGB-D camera on a tilt mechanism in the front to adjust the viewing angle. The RGB-D camera not only produces regular Red-Green-Blue (RGB) video images but also provides distance measurements. The remote control graphic user interface (GUI) on a tablet computer commands the robot motion, adjusts the suction power, controls camera view angle and LED lighting, and displays the first-person-view of the scene transmitted from the video camera through WiFi communication. The robot has a dimension of $16.5 \times 13 \times 8$ inches with self-weight 12 lbs. It can carry a payload up to 20lbs.

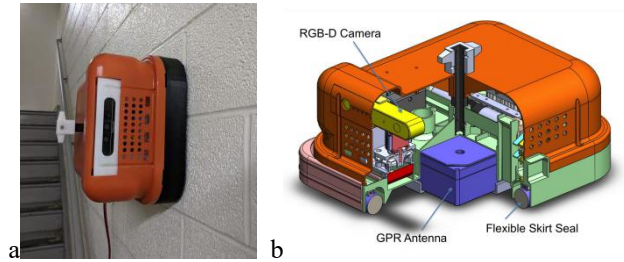


Fig. 2 The Wall-climbing robot prototype, a) Wall-climbing adhere to vertical wall, b) It carries an RGB-D sensor in front, and a GPR antenna at the bottom, inside a chamber enclosed by the flexible skirt seal.

3. Deep Neural Network and 3D Reconstruction for Concrete Inspection

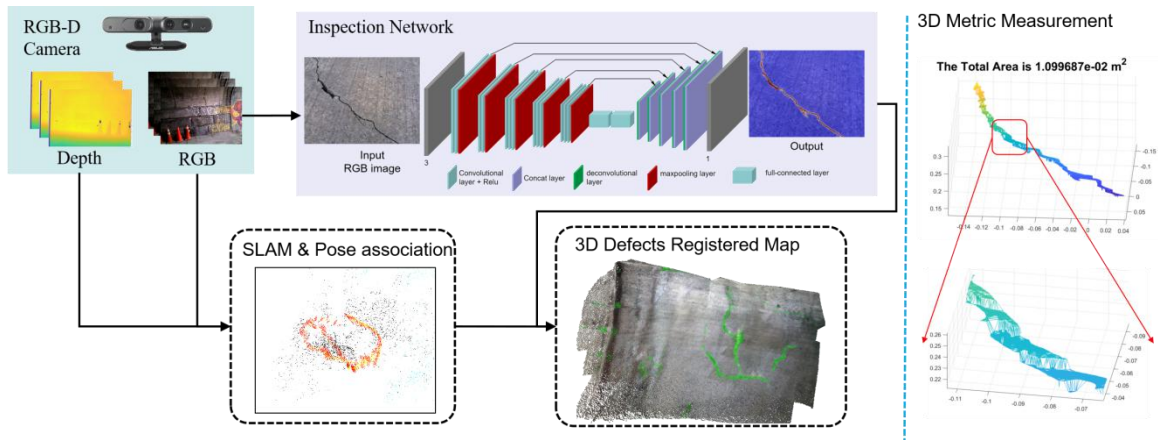


Fig. 3 The semantic 3D inspection system pipeline. The input from RGB-D sensor consists of RGB image and depth image. Then, our deep inspection network performs semantic detection of crack and spalling. Meanwhile, the visual SLAM system perform pose estimation and fuse the detection result to form a semantic 3D map as well as metric measurement.

To perform metric 3D inspection of the concrete structure, we propose to use an RGB-D camera based semantic reconstruction system as illustrated in Fig.3. For an RGB-D camera, it outputs both RGB image $I = \{(u_i, v_j, c) \in R^3 \mid 0 \leq i \leq n, 0 \leq j \leq m, c = 0,1,2\}$, and the corresponding depth image $D = \{d\}$. Then, we can obtain the point cloud at the each pose $T = (R, t)$ using pinhole model as,

$$\begin{bmatrix} X \\ Y \\ Z \end{bmatrix} = [R, t]^{-1} K[u, v] \quad (1)$$

Where $[X, Y, Z]$ denotes point cloud, $[R, t]$ denotes the rotation and translation at a location. K is the camera intrinsic parameter, and $[u, v]$ is a pixel in RGB image.

The pose $[R, t]$ is the current pose of the RGB-D camera, and it is obtained using ORB-SLAM2 algorithm (Mur-Artal Raul 2017). For ORB-SLAM2, it takes the RGB-D images as input. Given

current image frame I_p and previous image frame I_q , it first performs feature extraction and matching to obtain the matching feature pairs $F_{I_p} \rightarrow F_{I_q}$, then, the pose estimation can be achieved through the following optimization,

$$[R, t] = \arg \min_{R, t} \sum_{i \in \{1, \dots, N\}} L_p(F_{I_p}(i) - \pi(\|R \cdot F_{I_q}(i) + t\|_{\Sigma}^2)) \quad (2)$$

Where argmin denotes the linear regression process, $L_p()$ is the Huber Loss based cost function, and $\| \cdot \|_{\Sigma}$ denotes the covariance weighted sum toward a robust convergence. $\pi(\cdot)$ is inverse projection.

3.1 Inspection Neural Network

We develop a novel deep learning algorithm called Inspection network based on convolution neural network to detect the cracks and spallings on concrete structures. First, we create a pixel-level semantic dataset which includes 820 labeled images. To achieve robust modeling, we perform image flipping, rotation, and sub-cropping to do image augmentation for training as well as validation. The training on the dataset for InspectionNet is performed with 12,000 iterations for each defect type.

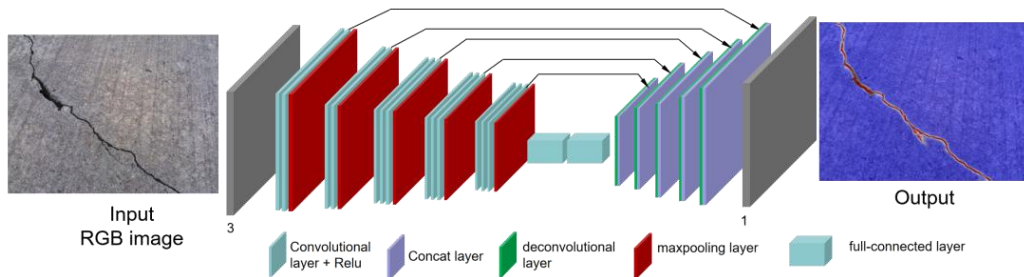


Fig. 4. Illustration of InspectionNet architecture for spalling/crack segmentation with pixel level accuracy.

Second, we adopt the U-net style deep neural network to perform end-to-end full pixel level segmentation as shown in Fig. 4. The InspectionNet consists of 25 layers, with the first 15 layers on the left are initialized based on VGG-16 as the pre-feature-extraction layers, and on the right side 10 convolutional layers (5 groups of deconvolution and convolution operations) to do upsampling. The defects are classified as either spallings or cracks with pixel level accuracy, enabling the quantitative measurement (e.g., the crack width, the area and depth of spallings) with the help of depth scale information obtained from the RGB-D camera.

3.3 Semantic 3D Defects Map

Since we have the pose $[R, t]$ and the inspection result over the images, we propose to use a 3D conditional random filter based fusion to obtain the semantic 3D map. The registration is performed using Equation (1) and Equation (2), meanwhile, we keep updating the color information coming from the inspection network. Thus, we can keep continuously updating the map when we move the RGB-D camera.

4. Experimental Study

4.1 Wall-climbing Robot Test

We conduct the adhesive force tests of the robot on the ground and smooth vertical surfaces, and the results are shown in Table.1. By selecting various adhesive suction motor speed (from 15% to 50%) in the percentage with respect to the maximum speed, we measure the pull-up adhesive force when the robot is placed on the ground surface. The pull-up force ranges from 4.62 to 31.62 Kg as shown in Table 1. In addition, we measure the vertical pull-down adhesive force (load capacity), which ranges from 1.3 to 10.5 Kg. When the adhesive suction motor speed is too low, the robot is not able to attach on vertical walls, its load carrying capability is marked as not available.

Table.1 Adhesive force testing for wall-climbing robot

Adhesive motor speed (percentage %)	15	20	25	30	35	40	45	50
Ground pull-up adhesive force Kg	4.62	5.62	8.22	11.02	16.42	24.5	28.95	31.62
Vertical pull-down adhesive force Kg	N/A	1.3	4.5	6.4	8.0	9.7	10.4	10.5

4.2 Inspection Field Test

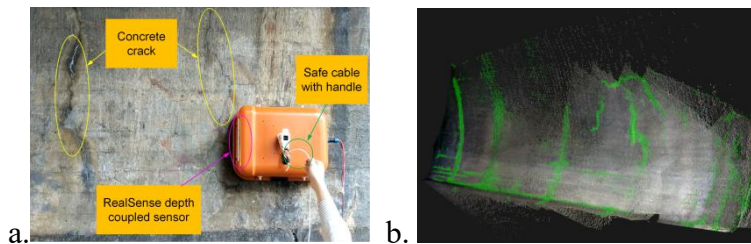


Fig. 5 Field testing results, a) deploy the robot on a vertical wall of a bridge tunnel, b) register the defects (green) in 3D point cloud map of the bridge tunnel.

We perform a field test to inspect the bridge tunnel at Riverside Drive and West 155th Street, New York City, NY 10032, whose results are illustrated in Figure 5. The inspection results (cracks in green) are registered in the concrete structure 3D model for better visualization and also provide a metric measurement for condition assessment and monitoring.

5. Conclusion

In this paper, we introduce a wall-climbing robot for SHM, using an RGB-D sensor and a neural network based 3D reconstruction method. Firstly, a state-of-the-art dataset with pixel-level labeling and an Inspection network were designed for semantic segmentation. Secondly, a visual odometry positioning and 3D reconstruction system is introduced. Finally, the visual inspection results were registered in the 3D model to provide metric information for concrete structure condition assessment. The field experiments show the effectiveness of our robotic inspection system with vertical mobility and effective visual inspection results. The future research plan is to investigate other NDE technologies (i.e., GPR and impact sounding) to detect and visualize subsurface deflection by integrating robotic control and SLAM with NDE signal processing technologies.

6. Acknowledgement

Financial support for this study was provided by the U.S. Department of Transportation, Office of the Assistant Secretary for Research and Technology (USDOT/OST-R) under Grant No. 69A3551747126 through INSPIRE University Transportation Center (<http://inspire-utc.mst.edu>) at Missouri University of Science and Technology. The views, opinions, findings and conclusions reflected in this publication are solely those of the authors and do not represent the official policy or position of the USDOT/OST-R, or any State or other entity.

References

- N. Gucunski (2015), "Condition assessment of bridge deck using various nondestructive evaluation (nde) technologies," *LTBP*, vol. 5, pp. 1–7, 2015.
- F. H. Administration (2014), "Specification for the national bridge inventory bridge elements," 2014.
- N. Y. D. of Transportation (2016), "Bridge inspection manual," January.
- F. H. Administration (2015), "Tunnel operations, maintenance, inspection, and evaluation (tomie) manual." .
- C. Koch, K. Georgieva, V. Kasireddy, B. Akinci, and P. Fieguth (2015), "A review on computer vision based defect detection and condition assessment of concrete and asphalt civil infrastructure," *Advanced Engineering Informatics*, vol. 29, no. 2, pp. 196–210.
- G. Li, S. He, Y. Ju, and K. Du (2014), "Long-distance precision inspection method for bridge cracks with image processing," *Automation in Construction*, vol. 41, pp. 83–95.
- R. Adhikari, O. Moselhi, and A. Bagchi (2014), "Image-based retrieval of concrete crack properties for bridge inspection," *Automation in construction*, vol. 39, pp. 180–194.
- M. R. Jahanshahi and S. F. Masri (2012), "Adaptive vision-based crack detection using 3d scene reconstruction for condition assessment of structures," *Automation in Construction*, vol. 22, pp. 567–576.
- R. S. Lim, H. M. La, and W. Sheng (2014), "A robotic crack inspection and mapping system for bridge deck maintenance," *IEEE Transactions on Automation Science and Engineering*, vol. 11, no. 2, pp. 367–378.
- P. Prasanna, K. J. Dana, N. Gucunski, B. B. Basily, H. M. La, R. S. Lim, and H. Parvardeh (2016), "Automated crack detection on concrete bridges," *IEEE Transactions on Automation Science and Engineering*, vol. 13, no. 2, pp. 591 – 599.
- H. M. La, N. Gucunski, K. Dana, and S.-H. Kee (2017), "Development of an autonomous bridge deck inspection robotic system," *Journal of Field Robotics*, vol. 34, no. 8, pp. 1489 – 1504,.
- N. Hallermann and G. Morgenthal (2014), "Visual inspection strategies for large bridges using unmanned aerial vehicles (uav)," in *Proc. of 7th IABMAS, International Conference on Bridge Maintenance, Safety and Management*, pp. 661 – 667.
- B. Li, K. Ushiroda, L. Yang, Q. Song, and J. Xiao (2017), "Wall-climbing robot for non-destructive evaluation using impact-echo and metric learning svm," *International Journal of Intelligent Robotics and Applications*, vol. 1, no. 3, pp. 255–270.
- Mur-Artal, Raul, and Juan D. Tardós (2017). "Orb-slam2: An open-source slam system for monocular, stereo, and rgb-d cameras." *IEEE Transactions on Robotics* 33.5 : 1255-1262.